
HydroGEN Seedling: Novel Chalcopyrites for Advanced Photoelectrochemical Water Splitting

Nicolas Gaillard

University of Hawaii / Hawaii Natural Energy Institute
2440 Campus Road, Box 368
Honolulu, HI 96822
Phone: (808)-956-2342
Email: ngaillard@hawaii.edu

DOE Manager: Eric Miller

Phone: (202) 287-5829
Email: Eric.Miller@ee.doe.gov

Contract Number: DE-EE0008083

Subcontractors:

- University of Nevada, Las Vegas, Las Vegas, NV
- Stanford University, Stanford, CA

HydroGEN Energy Materials Network nodes:

- Lawrence Livermore National Laboratory, Livermore, CA
- National Renewable Energy Laboratory, Golden, CO

Project Start Date: October 1, 2017

Project End Date: September 30, 2020 (subject to annual go/no-go decision)

Overall Objectives

The overarching goal of this project is to create a chalcopyrite-based, semi-monolithic, tandem hybrid photoelectrode device prototype that can operate for at least 1,000 hours with solar-to-hydrogen (STH) efficiency >10%. This effort is supported by advanced characterization and theoretical modeling to accelerate the development of materials and interfaces. Specifically, our program aims to:

- Develop high-throughput synthesis techniques to create efficient copper chalcopyrite-based materials with ideal optoelectronic properties for photoelectrochemical (PEC) water splitting,
- Identify appropriate surface treatments to prevent photocorrosion, improve surface energetics, and facilitate the hydrogen evolution reaction.

- Create a new method to integrate temperature-incompatible materials into a semi-monolithic PEC device structure.

Fiscal Year (FY) 2018 Objectives

- Identify the appropriate doping chemical element to passivate defects in chalcopyrite materials integrated on transparent conductive substrates.
- Improve chalcopyrite stability in aqueous electrolytes using ultra-thin protection layers, with a durability goal of 500 h continuous operation at a current density >5 mA/cm²,
- Develop a transparent/conductive adhesive to serve as binding material in the semi-monolithic integration scheme.

Technical Barriers

This project addresses the following technical barriers from the Hydrogen Production section of the Fuel Cell Technologies Office Multi-Year Research, Development, and Demonstration Plan¹:

- Materials efficiency (AE)
- Materials durability (AF)
- Integrated device configuration (AG)
- Synthesis and manufacturing (AJ).

Technical Targets

In Task 1, we evaluated the effect of alkali doping on point defects in CuGa₃Se₅ and developed a baseline “printing” process that will serve as a platform for future synthesis of Ga-free, wide-bandgap chalcopyrite candidates. In Task 2, we integrated non-precious catalytic-protecting layers and Cd-free buffers to enhance chalcopyrites’ durability and charge separation efficiency, respectively. Finally in Task 3, we developed transparent conductive epoxy/nanowire composites for semi-monolithic PEC device integration, aiming for optoelectronic properties comparable to that of vacuum-processed indium-doped tin oxide.

¹ <https://www.energy.gov/eere/fuelcells/downloads/fuel-cell-technologies-office-multi-year-research-development-and-22>

The status of this project's technical targets is documented in Table 1.

FY 2018 Accomplishments

Accomplishments during the current project period include:

- Modeling of copper-deficient chalcopyrite surfaces and their impact on energetics.
- Successful integration of CuGa_3Se_5 on F:SnO_2 (FTO) substrate via deliberate alkali doping.
- Chemical analysis of printed chalcopyrites via advanced spectroscopy techniques.
- Open-circuit voltage of 920 mV achieved with 1.8 eV $\text{CuGa}_3\text{Se}_5/\text{MgZnO}$ heterojunctions.
- Extended durability of CuGa_3Se_5 with WO_3 protective coating (400 hours so far tested).

Table 1. Progress Toward this Project's Technical Targets for FY 2018

Task #	Milestone Type	Milestone Description (Go/No-Go Decision Criteria)	Quarter	Status
1	Milestone	A printed polycrystalline chalcopyrite thin film material made of grains at least 500 nm across and with impurity concentration less than 15%.	Q1	100%
3	Milestone	Produce a nanowire and epoxy based composite demonstrating a sheet resistance below 200 Ω/sq and transparency > 70%.	Q2	100%
2	Milestone	Stabilized chalcopyrite photocathode that retains 90% of its copper content after 100 hrs of continuous operation to achieve an initial photocurrent density of 8 mA/cm^2 under simulated AM1.5G illumination.	Q3	100%
1	Go/No-Go (1/2)	A solution-processed $\text{CuIn}(\text{S,Se})_2$ -based PV device with a short-circuit photocurrent density corresponding to at least 70% of the absorber's theoretical limit and free-electron losses ($E_g - \text{Voc.q}$) less than 600 mV.	Q4	95%, on track
2	Go/No-Go (2/2)	Demonstrate 500 hrs stability in a photoelectrode operating under simulated AM1.5G illumination at a fixed potential that achieves an initial photocurrent of 8 mA/cm^2 and does not drop below 5 mA/cm^2 over the duration of the test.	Q4	85%, on track

INTRODUCTION

Our multidisciplinary program combines advanced synthesis techniques, unique characterization, and theoretical approaches to improve the efficiency and durability of chalcopyrite-based hybrid photoelectrode devices, with the final goal of producing a chalcopyrite-based, semi-monolithic device with at least 10% STH efficiency.

APPROACH

We aim to advance the performance of previously identified wide-bandgap chalcopyrite materials through alkali doping, as well as develop and test the water-splitting viability of the next generation of chalcopyrites. We also see unrealized potential to improve the PEC/electrolyte interface energetics and stability, which is addressed by investigating alternative buffer materials and protective layers. Finally, to avoid the heat-stress issues facing all-chalcopyrite monolithic tandem devices, we investigate a semi-monolithic structure, which will utilize a transparent conductive bonding polymer and exfoliation technique to avoid exposing the bottom photovoltaic (PV) driver in these devices to the high temperatures required for wide-bandgap chalcopyrite synthesis.

RESULTS

Task 1: Modeling and Synthesis of Chalcopyrite Photocathodes

This first year, we investigated the thermodynamic stability of chalcopyrite-derived compounds and competing phases that can form during fabrication and processing of larger-bandgap chalcopyrites. Specifically, we focused on the properties of Cu-deficient (ordered-vacancy compound, or OVC) phases and alkali-derived phases and how they may influence device performance. For example, the existence of OVC-type phases such as CuIn_5Se_8 has long been believed to form in certain processing conditions and influence the resulting device performance via changing the nature of the various heterostructure interfaces formed. Understanding the role of these compounds and under what regimes they are expected to form is key to tuning process conditions that lead to expected performance. This knowledge is additionally helpful in identifying whether the formation of such phases should be explicitly targeted in synthesis processes. In Figure 1 we show the calculated phase diagrams for the larger-bandgap CuGaS_2 absorbers that exhibit a large sensitivity of the qualitative features of OVC-phase formation depending on details of the calculations. This illustrates the complexity in identifying under which conditions these phases are expected to be present.

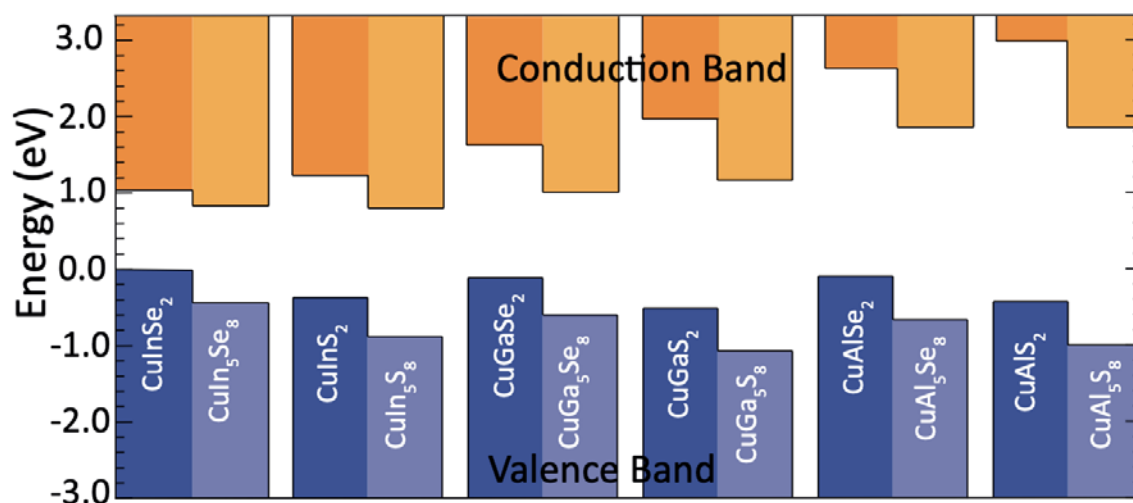


Figure 1. Effect of ordered vacancy compounds on chalcopyrites band offsets

Following these modeling efforts, we studied the effects of alkali metal doping in CuGa_3Se_5 OVC materials grown on glass substrates containing various amount of alkali and coated with Mo back contact. This study

revealed that best PEC performances are obtained on CuGa_3Se_5 absorbers grown on Na-containing SLG substrates. To test the PEC performance of CuGa_3Se_5 photocathodes in a transparent top cell configuration, absorbers were grown directly on FTO back contacts (Pilkington), which include a Na-diffusion barrier between the soda-lime glass and FTO layer. Introducing 15 nm of NaF post-deposition greatly improved the saturated photocurrent density (Figure 2). Moving to thicker pre-deposited NaF appeared also to increase the saturated photocurrent density and photocurrent onset further (up to 0.4 V versus reversible hydrogen electrode, which is the best value ever observed for NREL's bare CuGa_3Se_5). No buffers or catalyst layers were applied to these films yet, and these PEC characteristics are approaching those of the best baseline CuGa_3Se_5 films grown on Mo. These are promising results for the development of tandem water-splitting devices.

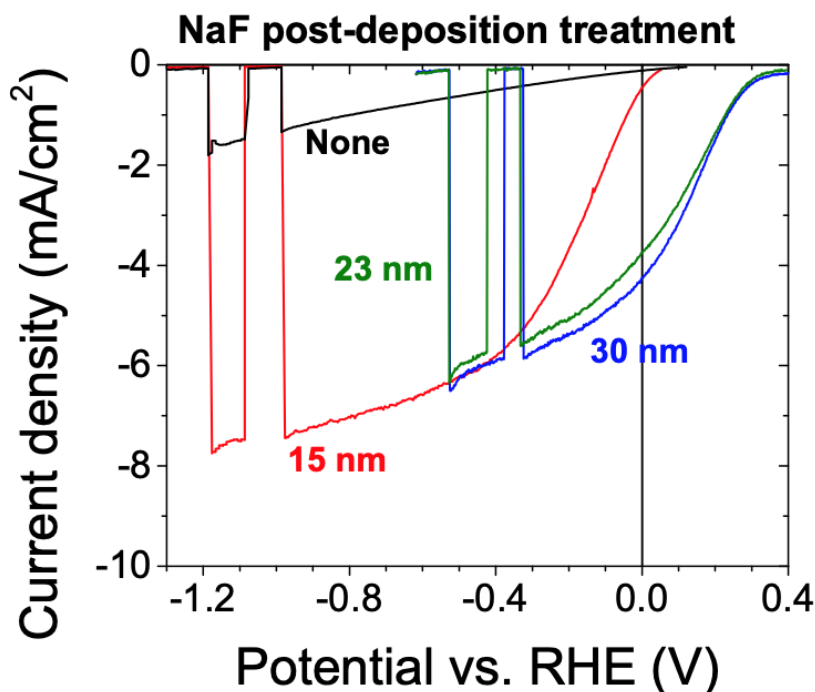


Figure 2. Linear sweep voltammetry characteristics of transparent photocathodes (glass/FTO/ CuGa_3Se_5) with different thicknesses of NaF

Task 2: Interface Engineering for Enhanced Efficiency and Durability

In the first year of this project, we focused on characterizing the electronic and chemical properties of samples produced using liquid processing (printable inks) using X-ray emission spectroscopy at Lawrence Berkeley National Laboratory. Two sample sets were analyzed: two CuInS_2 as-deposited samples and two $\text{CuIn}(\text{S},\text{Se})_2$ selenized samples. The former samples were taken at an intermediate step of the production process—in the full process, they serve as precursors to the latter sample. One sample set was made fully in air (ink formulation and coating), while the other sample set was synthesized with ink formulated in a glovebox using high-performance liquid chromatography (HPLC)-grade methanol and spin-coated in air. The results of the sulfur $L_{2,3}$ X-ray emission spectroscopy study revealed that both CuInS_2 “HPLC” and CuInS_2 “in-air” exhibited dominant transitions typical of sulfur in a sulfide environment. Also, spectral features of S-In, S-Cu, and S-O bonding were observed in these samples. The S-In and S-Cu peaks also appear in the $\text{CuIn}(\text{S},\text{Se})_2$ “HPLC” and $\text{CuIn}(\text{S},\text{Se})_2$ “in-air” spectra, which is expected because CuInS_2 is a precursor of the $\text{CuIn}(\text{S},\text{Se})_2$ samples. Nevertheless, we ruled out the presence of S-O bonds in these selenized samples. Overall, at the near-bulk surface, all four samples have similar chemical environments of sulfur, representing a high-quality $\text{CuIn}(\text{S},\text{Se})_2$ environment. Furthermore, X-ray photoelectron spectroscopy data has been taken at University of Nevada, Las Vegas to analyze the chemical surface structure of these samples. Over the course of the project

year, we find a significant reduction of carbon- and oxygen-containing adsorbates and impurities, especially when comparing sample sets processed in the glovebox to those synthesized in air.

During FY 2018 we also studied alternative buffer materials via combinatorial RF sputtering. Specifically, we integrated Ga-doped $\text{Zn}_{1-x}\text{Mg}_x\text{O}$ buffers on CuGa_3Se_5 -based PV devices with different configurations. Devices integrated without CdS (replaced with $\text{Zn}_{1-x}\text{Mg}_x\text{O}$) didn't exhibit any quantifiable current generation, whereas those combining both $\text{Zn}_{1-x}\text{Mg}_x\text{O}$ and CdS exhibited higher device voltage and higher current output compared to the baseline device, indicating favorable conduction band offset. Overall quantum efficiency of the devices was improved, and the long wavelength carrier collection increased with increasing Mg concentration, indicating reduction in carrier recombination. Promising results were achieved by combining Cd^{2+} partial electrolyte (PE) treatment with ZnMgO. The CuGa_3Se_5 device performances were found to be dependent on the temperature and the duration of the Cd^{2+} PE treatments. Comparative quantum efficiency of different device configurations (Figure 3) show that replacing CdS with Cd^{2+} PE/ $\text{Zn}_{1-x}\text{Mg}_x\text{O}$ as the window layer improves the carrier collection in the short wavelengths due to the higher bandgap of ZnMgO. Open circuit voltage up to 920 mV was measured, which can be significant for PEC water splitting applications.

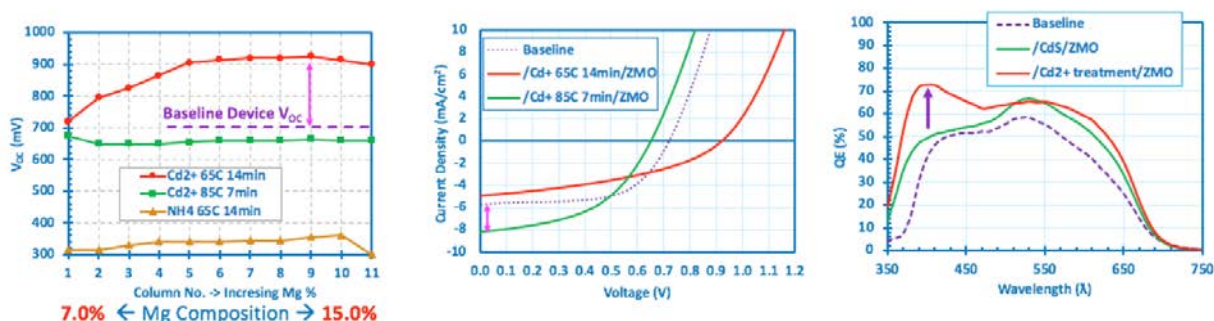


Figure 3. Solid-state performance for CdS-free $\text{CuGa}_3\text{Se}_5/\text{Zn}_{1-x}\text{Mg}_x\text{O}$ devices with different surface treatments

Finally, we developed protective and catalytic coatings for chalcopyrite photocathode operation in acidic electrolyte conditions and quantified the degradation of these protected devices. Linear sweep voltammograms measured on three CuGa_3Se_5 photocathodes coated with 3-nm-thick WO_3 protective layer and nanoparticulate Pt catalyst demonstrated good photocurrent onset at +0.1 V versus reversible hydrogen electrode or greater and reached a saturation photocurrent density (j_{ph}) of at least -6 mA cm^{-2} under 1 Sun illumination. Subsequent chronoamperometric (CA) durability tests were performed on these same devices with the potential being held in the light-limited region under constant illumination. Notably, two devices have reached 85% of Phase 1 go/no-go durability target (see Table 1 for details). Additionally, we measured the degradation of a CuGa_3Se_5 absorber film protected with a 3-nm atomic layer deposition film of WO_3 using inductively coupled plasma mass spectrometry analysis. Our study shows that the dissolved quantity of copper in solution is less than 5.6% over 100 h of testing, satisfying the Q3 milestone.

Task 3: Hybrid Photoelectrode Device Integration

During FY 2018, we focused on the development of a transparent conductive binder for semi-monolithic hybrid device integration. With this approach, we propose to solve process compatibility issues between material classes by bonding a chalcopyrite photoelectrode onto a fully processed PV driver. Excellent results were achieved with composites made of silver nanowires (AgNWs). In this experiment, AgNWs (L: $27 \pm 23 \text{ } \mu\text{m}$, diam: $72 \pm 21 \text{ nm}$) suspended in isopropanol (2.55 wt%) were first dispersed in cellulose (0.96 wt%). Then, roughly 100 μL of the AgNWs/cellulose solution was spin coated onto a SLG substrate for 45 seconds at 800 rpm and subsequently annealed on a hot plate in air at 100°C . Figure 4 presents a picture of the resulting SLG/AgNWs transparent sample as well as a top view scanning electron micrograph. One can see that the AgNWs are well dispersed and form an interconnected network with enough separation in between to allow light transmission. The latter was confirmed by ultraviolet-visible analysis, showing transmission over 92% in

the 350–1,200 nm range. The sheet resistance of this sample, measured by 4-point probe technique, was 22 ohm/square, exceeding the Q2 milestone.

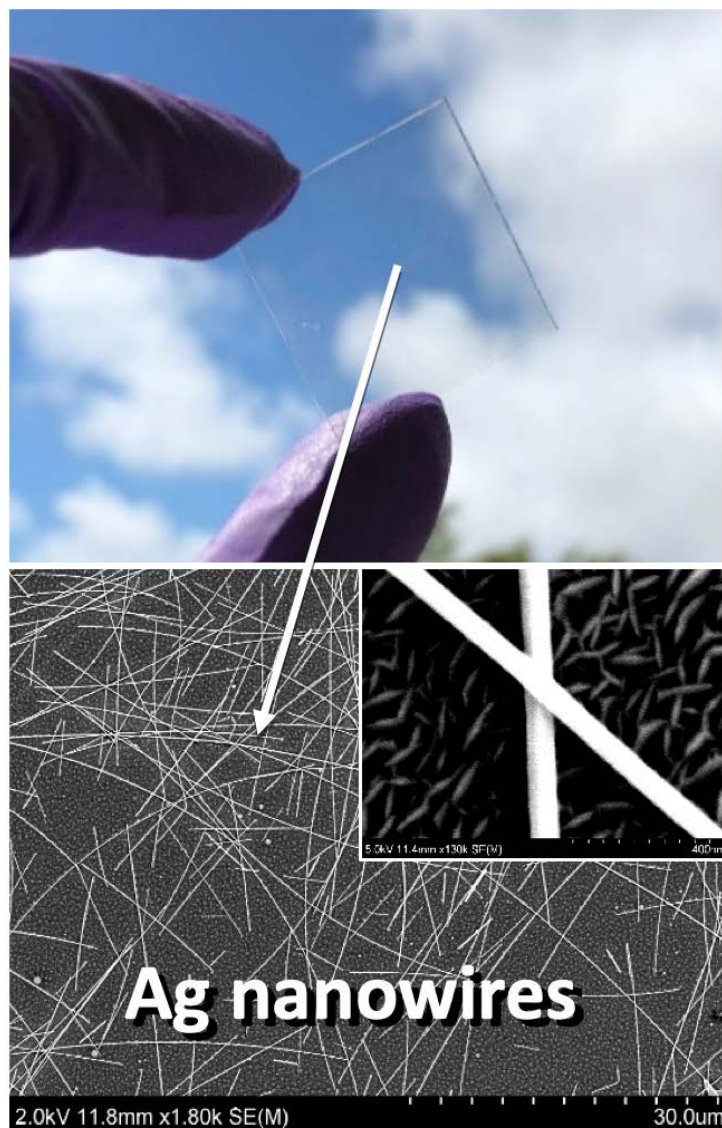


Figure 4. Optical image and scanning electron micrograph of a conductive transparent adhesive made with silver nanowires

CONCLUSIONS AND UPCOMING ACTIVITIES

- Further validate protection with WO_3 film, targeting 500 h of continuous operation.
- With help from advanced spectroscopy, improve chalcopyrites solution processing, aiming for high-efficiency solid-state CuInSe_2 devices.
- Continue the development of ZnMgO buffers, targeting over 1 V open circuit voltage.
- With help from theory, further develop chalcopyrites alkali doping to create highly efficient photocathodes on transparent substrates.